

## **LOWER FREQUENCY LIMIT OF CARBON NANOTUBE ANTENNA**

**A. M. Attiya**

Electronics Research Institute, Microwave Engineering Department  
El-Tahreer St., Dokki, Giza, Egypt

**Abstract**—Carbon nanotubes are characterized by slow wave propagation and high characteristic impedance due to the additional kinetic inductive effect. This slow wave property can be used to introduce resonant dipole antennas with dimensions much smaller than traditional half-wavelength dipole in Terahertz band. However, this property has less effect at lower frequency bands. This paper introduces the physical interpretation of this property based on the relation between the resonance frequency and the surface wave propagation constant on a carbon nanotube. This surface wave propagation is found to be characterized by high attenuation coefficient at low frequency bands which limits using carbon nanotube as an antenna structure at these frequencies.

### **1. INTRODUCTION**

Carbon nanotubes (CNT) were discovered experimentally in early 1990s by Iijima [1]. Since this date these structures have been fertilized fields of research due to their unique featured physical properties. CNT can be considered as a rolled graphene sheet. They are classified to single wall or multi-wall CNTs according to the number of these rolls. They are also classified according to the axis around which the graphene sheet is rolled.

On the other hand, the ac conductivity and electromagnetic wave interaction of the conducting CNTs have also important features compared with traditional conductors like copper wires of the same size. Slepyan et al. [2,3] introduced the earliest study of electromagnetic wave interaction with CNT. Their study included the dc and ac conductivity of single wall CNTs and surface wave and

---

Corresponding author: A. M. Attiya (aattiya@ksu.edu.sa).

leaky wave propagation along these nanotubes. On the other hand, Miyamoto et al. [4] studied the inductive effect specifically due to the chiral structure of these nanotubes. Instead of effective boundary condition and surface conductivity, Mikki and Kishk [5] presented a microscopic model to derive the Green's function that represents the interaction of electromagnetic waves with single wall CNT based on the potential at each atom in its periodical atomic structure. The main problem of this method is that the resulting formulation is much more complicated to be included in a simple simulation code.

Hanson [6] presented a detailed comparison between the ac conductivity of different single wall CNTs and 2D ac conductivity of copper. From his results it can be concluded that the ac conductivity of these CNTs are characterized by negative imaginary part compared with copper. This negative imaginary part corresponds to an inductive effect. This inductive effect is due to the stored kinetic energy in the CNT structures. Burke [7,8] used electron fluid model to introduce an equivalent circuit model for CNT transmission line section. He introduced additional kinetic inductance and quantum capacitance effects that represent the ac conductivity behavior of CNT transmission line section. The details of deriving these additional circuit parameters from the ac conductivity of CNTs are discussed in Refs. [9–12]. This kinetic inductance is found to be much larger than the traditional magnetostatic inductance of transmission line section. On the other hand, the quantum capacitance is nearly of the same order of the electrostatic capacitance of the transmission line section. This property has two main effects on electromagnetic wave propagation along the CNT transmission line; slow wave propagation and high characteristic impedance.

The slow wave propagation along conducting CNTs and the high conductivity compared with metallic conductors like copper make these structures competitive candidates for high frequency applications where the dimensions should be comparable to the propagation wavelength. This property can be of great importance in reducing the size of antenna and passive circuits. This is similar to the traditional technique of adding small coils in the arms of the dipole antenna to reduce its resonance length [13]. However, the coil in this case is distributed along all the antenna structure. This advantage was the motivation for different authors to study the possibility of using these CNTs as antennas [6, 14–17].

Burke et al. [16] presented a detailed study on CNT dipole antenna based on simple transmission line approximation. They assumed that the antenna is simply a flared part of a transmission line section where the wave travels approximately with the same velocity on it. This

wave velocity on the CNT transmission line equals nearly the Fermi velocity in CNT. They mentioned that the wave velocity would be slightly affected by the flaring since it depends only on the variation of the capacitance effect which is sensitive to the log of the distance between the two arms. Thus, based on this assumption, they showed that a lossless CNT of length  $150\ \mu\text{m}$  would be resonant at 10 GHz which corresponds to the half plasmonic wave length at this frequency. They followed up this assumption to present other properties of CNT dipole antenna like input impedance, mutual impedance, radiation resistance, directivity and efficiency. They also presented an integral equation representation based on the transmission line equivalent circuit parameters to obtain the exact current distribution on the CNT instead of approximating it as a sinusoidal standing wave pattern.

On the other hand, Hanson [6] presented an integral equation based on the macroscopic surface conductivity of the CNT instead of the equivalent circuit parameters of the CNT transmission line. Similar formulations are presented by other authors [18, 19].

However, the main problem in using CNT as a TL section or an antenna structure is the corresponding high characteristic impedance. To reduce the characteristic impedance of CNT TL, CNT bundles were introduced [20, 21]. This CNT bundle is a set of parallel single wall CNT. In Refs. [20, 21] they showed that the slow-wave coefficients for azimuthally symmetric guided waves increase with the number of metallic CNTs in the bundle, tending for thick bundles to unity, which is characteristic of macroscopic metallic wires. Thus, there is a compromise between reducing the length of the resonant bundle dipole and reducing the resonant input impedance.

The points which are required to be clarified can be summarized in two main points; (i) Is CNT bundle suitable to be used as an antenna in lower Giga Hertz range by just scaling the dimension? And (ii) what is the real mechanism of wave propagation along the nanotube bundle in this range? These points are discussed in this paper through two directions; integral equation representation of CNT bundle and surface wave propagation along a CNT. By comparing the results of the integral equation and the surface wave propagation of CNT bundle, the resonance behavior of CNT bundle and the lower frequency limit of this resonance are clarified. The present analysis is based on SI units and harmonic time dependence  $e^{j\omega t}$ .

## 2. THEORY

### 2.1. Basic Parameters of Single Wall Carbon Nanotube

Single wall Carbon can be considered as a rolled graphene sheet. The lattice of graphene sheet is a honeycomb hexagonal shape. The spacing between two adjacent carbon atoms in graphene sheet is  $b = 0.142$  nm. CNTs are defined by the vector that describes the circumference of the rolled graphene sheet. This vector is simply the vector summation of integer multiples of the two lattice basis vectors. The dc conductivity of CNT depends on these integer number multiplications;  $m$  and  $n$ . Armchair CNTs of two equal vector indices ( $m = n$ ) are always conducting. In this case the radius of the of tube is  $a = 3mb/2\pi$ . This paper is based only this armchair configurations. Other configurations like zigzag can also be conductors at specific case or semiconductors in other case.

The conductivity of CNT depends mainly on it chirality. This conductivity is divided into two parts; intraband and interband conductivities [22]. Interband transitions have more significance in optical frequencies. Thus, the present analysis is mainly depending on intraband conductivity of an armchair CNT which can be approximated for small radius armchair CNT where  $m \leq 50$  as [6]:

$$\sigma_{zz}^{cn} \approx -j \frac{2e^2 v_F}{\pi^2 \hbar a (\omega - jv)} \quad (1)$$

where  $v_F \approx 9.71 \times 10^5$  m/s is the Fermi velocity of CNT;  $v = \tau^{-1}$  is the inverse of the electron relaxation time in CNT lattice  $\tau \approx 3$  ps;  $\omega$  is the operating frequency;  $e$  is the electron charge;  $\hbar$  is the reduced Planck's constant. For a CNT bundle composed of  $N$  identical tubes arranged as a cylindrical shell of radius  $R$  as shown in Fig. 1, the effective axial surface conductivity of this shell can be approximated by [21]:

$$\sigma_{zz}^b \approx \frac{N \sigma_{zz}^{cn} a}{R} \quad (2)$$

### 2.2. Integral Equation Representation of Carbon Nanotube Bundle

The integral equation representation of electromagnetic wave interaction with CNT was first discussed by Hanson [6]. Different authors have followed up his analysis with slight modification to include second order effects like the curvature of the CNT surface. The basic idea of integral equation representation for CNT is based on using Hallén's

integral equation with adding the effect of surface conductivity as follows:

$$\int_{-L}^L \left( \frac{e^{-jk_o\sqrt{(z-z')^2+R^2}}}{\sqrt{(z-z')^2+R^2}} + \frac{1}{Z_o\sigma R} e^{-jk_o|z-z'|} \right) I(z') dz' = C \cos k_o z - j \frac{4\pi\omega\varepsilon_o}{2k_o} \sin k_o|z-z_0| \tag{3}$$

where  $R$  is the radius of the dipole ( $R = a$  for single nanotube), and  $\sigma$  is the effective surface conductivity of the dipole,  $z_0$  is the location of the feeding point,  $C$  is a constant that would be determined to satisfy the current vanishing at the edges of the dipole, and  $L$  is the half length of the dipole. The main difference in this integral equation lies in the second term of the integrand in the left hand side. This integral equation can be solved numerically by using method of moments to find out the current distribution and subsequently the input impedance, radiation pattern, radiation efficiency and other antenna parameters. Details of solving this integral equation numerically by using method of moments can be found in [23].

### 2.3. Surface Wave on Carbon Nanotube

Another approach for studying electromagnetic wave interaction with CNT (single or bundle) is to study guiding wave properties of this structure [24]. Since the effective conductivity lies only on the axial direction, the surface wave component would be mainly TM wave. Thus, the total field can be represented in terms of the axial TM *Hertzian* potential  $\Pi_e$  as follows:

$$\vec{E} = \nabla(\nabla \cdot \Pi_e) + k_0^2 \Pi_e \tag{4a}$$

$$\vec{H} = j\omega\varepsilon_o \nabla \times \Pi_e \tag{4b}$$

where TM *Hertzian* potential is determined by solving the wave equation

$$\nabla^2 \Pi_e + k_0^2 \Pi_e = 0 \tag{5}$$

For cylindrical configuration as in the case of CNT, the general solution of wave equation is Bessel function. The field inside the cylinder is finite in the range  $0 \leq \rho \leq R$ . Thus, the field in this region is represented by Bessel function of first kind. On the other hand, the field outside the cylinder should be finite at  $\rho = R$  and is exponentially decaying as  $\rho > R$ . Thus, the field in this region is represented by

Hankel function of second kind. Hence, the general solution of the TM *Hertzian* potential in CNT (single or bundle) can be represented as:

$$\Pi_e = A\vec{a}_z \begin{cases} J_n(\kappa\rho)H_n^{(2)}(\kappa R) \\ J_n(\kappa R)H_n^{(2)}(\kappa\rho) \end{cases} e^{-j\gamma z} e^{-jn\phi} \quad \begin{matrix} \rho \leq R \\ \rho \geq R \end{matrix} \quad (6)$$

By using this *Hertzian* potential in Eq. (4) and applying the boundary condition

$$J_z = \sigma_{zz}E_z(R) = -\lim_{\delta \rightarrow 0} [H_\phi(R + \delta) - H_\phi(R - \delta)] \quad (7)$$

one can obtain the dispersion equation for surface wave propagation on a CNT as follows:

$$\left(\frac{\kappa}{k_o}\right)^2 J_n(\kappa R)H_n^2(\kappa R) = \frac{2}{\pi\sigma_{zz}Z_o k_o R} \quad \text{where } \text{Im}(\kappa) \leq 0 \quad (8)$$

The longitudinal propagation constant is given by:

$$\gamma = \sqrt{k_o^2 - \kappa^2} \quad \text{where } \text{Im}(\gamma) \leq 0 \quad (9)$$

It would be useful here to study the limit of the above dispersion equation for the zero order mode at small argument limit. In this case the Bessel function combination of the right hand side can be approximated as:

$$J_0(\kappa R)H_0^{(2)}(\kappa R) \approx \left(1 - j\frac{2}{\pi}[\ln(\kappa R/2) + 0.577215]\right) \quad (10)$$

Unlike Bessel function, the logarithmic function in the right hand side of Eq. (10) can be represented by a slowly convergent series for small argument. However, for Giga Hertz frequency band, the average value of this logarithmic function is nearly around minus ten. Thus, an approximate value of the zero order mode complex surface wave propagation coefficient along a CNT is given by:

$$\gamma \approx k_o \sqrt{1 - \frac{1}{\sigma_{zz}Z_o k_o R (\pi/2 + j10)}} \quad (11)$$

It can be noted that, by increasing the longitudinal conductivity of the tube, the surface wave propagation constant approaches the free space propagation constant.

## 2.4. Quasi TEM Carbon Nanotube Transmission Line

To verify the difference between feeding CNT transmission line and wave propagation along the arms of nanotube antenna, it is required to study the quasi TEM wave propagation along CNT transmission line. CNT transmission line above a PEC ground plane was studied by using transmission line equation including the effect of the conductivity of the CNT [9, 10]. This analysis is based on an equivalent  $RLC$  circuit per unit length for this transmission line configuration. This equivalent circuit can be used directly to obtain the complex propagation constant of CNT transmission line above a PEC ground plane as follows:

$$j\gamma = j\beta - \alpha = \sqrt{j\omega C (j\omega L_{eff} + R_{eff})} \quad (12a)$$

where

$$L_{eff} = \frac{L + L_k}{1 + C/C_Q}, \quad (12b)$$

$$R_{eff} = \frac{R_Q}{1 + C/C_k}, \quad (12c)$$

here  $L$  and  $C$  represent the magnetostatic inductance and electrostatic capacitance per unit length respectively. For a cylindrical CNT bundle transmission line above a PEC ground plane, these parameters can be obtained analytically as follows [25]:

$$L = \frac{\mu_0}{2\pi} \cosh^{-1} \left( \frac{t}{R} \right) \quad (13a)$$

$$C = \frac{2\pi\epsilon_0}{\cosh^{-1} \left( \frac{t}{R} \right)} \quad (13b)$$

where  $t$  and  $R$  are the height of the CNT bundle transmission line above the ground plane and the radius of the CNT bundle respectively. On the other hand,  $L_k$ ,  $C_Q$  and  $R_Q$  correspond to kinetic inductance, quantum capacitance and resistance per unit length respectively. These parameters are given by [7–10]:

$$L_k = \frac{h}{8Ne^2v_f} \quad (14a)$$

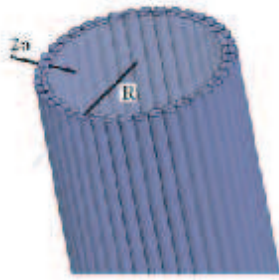
$$C_Q = N \frac{8e^2}{hv_f} \quad (14b)$$

$$R_Q = \frac{h}{8Ne^2} \quad (14c)$$

where  $N$  is the number of tubes in the bundle;  $v_f$  is the Fermi velocity of CNT structure;  $h$  is Planck's constant;  $e$  is the electron charge.

### 3. RESULTS AND DISCUSSIONS

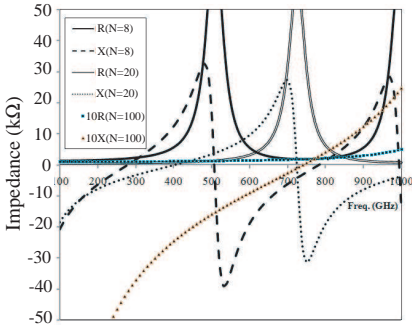
In this section different results of CNT bundles at different frequency ranges are presented to study the possibility of scaling these antenna configurations from Terahertz frequency band to Giga Hertz frequency band. The present results are based on armchair CNT of configuration  $m = n = 40$ . For this configuration, the radius of the CNT is  $a = 2.7$  nm. For a closely backed bundle composed of  $N$  CNT arranged in a single circular shell as shown in Fig. 1, the radius of the bundle is  $R = 2Na/\pi$ .



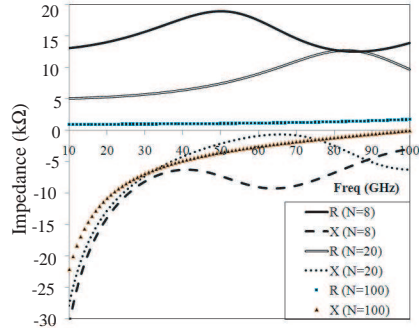
**Figure 1.** Geometry of a Cylindrical CNT Bundle composed of one circular shell.

Figure 2 shows the input impedance of a dipole of a CNT bundle for different values of  $N$ . The length of the dipole is assumed to be  $30 \mu\text{m}$ . It can be noted that the first resonance of this configuration that corresponds to a half-guided-wave length dipole for the case  $N = 8$  occurs nearly at 280 GHz where the resonant impedance is nearly 2100 Ohms. By comparing this length with free space half-wave at this frequency it can be shown that this CNT antenna has a reduction scale factor of nearly 0.056 compared with traditional half-wave length dipole. Increasing the number of nanotubes in the bundle decreases the total surface impedance of the dipole. This has two effects, increasing the resonant frequency for a specific length and decreasing the resonant impedance as shown in the case where  $N$  is increased to twenty. In this case the first resonance frequency is 404 GHz and the resonance impedance is 840 Ohms. In this case the scale reduction factor is nearly 0.081. For a hundred nanotube bundle of the same length, the resonant frequency would be 740 GHz and the resonance impedance would be 174 Ohms. In this case the scale reduction factor is nearly 0.15.

By scaling these antenna configuration ten times such that the length of the dipole would be  $300 \mu\text{m}$ , the results shown in Fig. 3 are



**Figure 2.** Input impedance of a bundle dipoles of  $L = 30 \mu\text{m}$ . The bundle is composed of armchair CNTs with lattice parameters  $m = n = 40$ . Numbers of nanotubes in the bundles are  $N = 8$ ,  $N = 20$  and  $N = 100$ .



**Figure 3.** Input impedance of a bundle dipole of  $L = 300 \mu\text{m}$ . The bundle is composed of armchair CNTs with lattice parameters  $m = n = 40$ . Number of nanotubes in the bundle is (a)  $N = 8$ , (b)  $N = 20$  and (c)  $N = 100$ .

obtained. This results shows that there is no resonance in this case although the general behavior of the impedance is nearly the same as in Fig. 2 with frequency scaling of one tenth. This means that simple scaling of CNT antenna would not introduce the same properties in another frequency band. It should be noted that the radius of the dipole does not play a critical role in this case since it is very small compared with the operating frequency in all cases. It can also be noted that the input impedance of antenna at 10–100 GHz band is always capacitive load. This means that the advantage of antenna size reduction that is obtained by using CNT in 100–1000 GHz band cannot be directly transformed to lower frequency range by simple scaling of the antenna structure.

By introducing another scaling factor of ten such that the length of the dipole would be  $3000 \mu\text{m}$ , the input impedances of dipole antenna configurations for the two cases where  $N = 8$  and  $100$  are obtained is shown in Fig. 4. It can be noted that the behavior of the input impedance of these antenna configurations in the frequency range from 1 to 10 GHz is completely different from those of Fig. 2 with taking into consideration the scaling factor. In this case the real part of impedance is monotonically decreasing with frequency increase and the reactive part is always capacitive and it is monotonically increasing with frequency increase too.

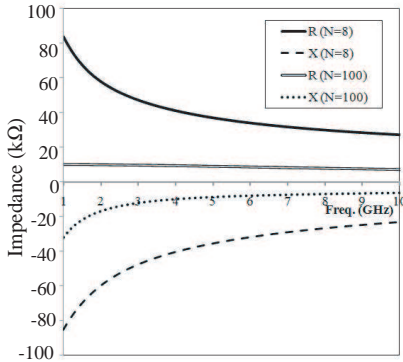


**Figure 4.** Input impedance of a bundle dipole of  $L = 3000 \mu\text{m}$ . The bundle is composed of armchair CNTs with lattice parameters  $m = n = 40$ . Number of nanotubes in the bundle is (a)  $N = 8$ , (b)  $N = 100$ .

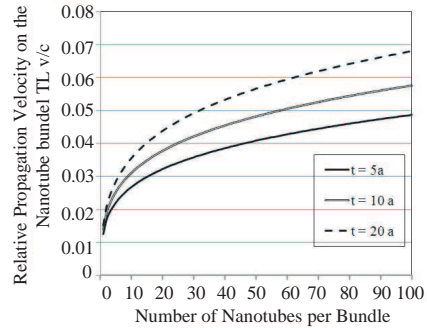


**Figure 5.** Wave velocity compared with free space wave propagation of a quasi-TEM TL CNT bundle above a PEC ground plane as a function of  $N$ . The separation between the bundle and the ground plane is  $5a$ ,  $10a$  and  $20a$ .

According to the simple theory of center-fed dipole, it can be approximated as a flared transmission line section with open circuit termination [25]. This open circuit termination introduces a standing wave pattern on this transmission line section. For the case of a perfect conducting transmission line in free space, the propagation constant on the transmission line and the flared section would be the free space propagation constant. The resonance of the dipole occurs when the standing wave pattern on the arms of the dipole introduces peak current at the feeding point of the dipole. The first current peak occurs when the length of the flared section equals nearly one-fourth of the propagation wave length which means that the total dipole length would be half-wave length. The main misleading part in this interpretation is that the wave propagation on the transmission line and the flared section of perfect conducting transmission line are the same in free space.

Burke et al. [16] introduced quantitative theory of nanotube antenna. In their method, they assumed that the electromagnetic wave would propagate with the same propagation constant at the feeding nanotube transmission line. Fig. 5 shows the calculated  $v/c$  for a CNT bundle TL above a ground plane as a function of the number of nanotubes in the bundle. The separation between the bundle and

the ground plane is assumed to be three different values;  $t = 5a$ ,  $10a$  and  $20a$  where  $a$  is the radius of a single nanotube. For the case where  $t = 10a$ , the propagation wave velocity compared with free space wave velocity in this case for bundles of  $N = 8$ ,  $20$  and  $100$  would be  $0.03$ ,  $0.0378$  and  $0.0576$  respectively. By comparing these wave velocities with the corresponding scale reduction factors for the dipole of Fig. 2, it can be noted that, this quasi-TEM wave velocity is not related to the resonant length of the CNT bundle dipole antenna which is calculated by full wave analysis. It can also be noted from Fig. 5 that changing the separation between the CNT bundle and the ground plane would not introduce a significant effect on the order of these values for the CNT bundle TL. Thus, it can be concluded that the mechanism of wave propagation on the arms of the dipole is different from the propagation on the feeding transmission line in this case.

The previous result was the motivation here to look for another explanation for the mechanism of wave propagation along the dipole arms and also to introduce a physical interpretation for the results shown in Figs. 2–4. The appropriate mechanism in this case is the surface wave propagation on the dipole arms. It should be noted that surface wave propagation velocity on a perfect conducting tube in free space is the same as free space propagation velocity as it is shown in Eq. (11). Thus, the surface wave interpretation does not conflict with the basic theory of perfect conducting dipole in free space [25]. Fig. 6 shows the surface wave propagation on the same bundle configurations. It can be noted that the surface wave velocity compared with the free

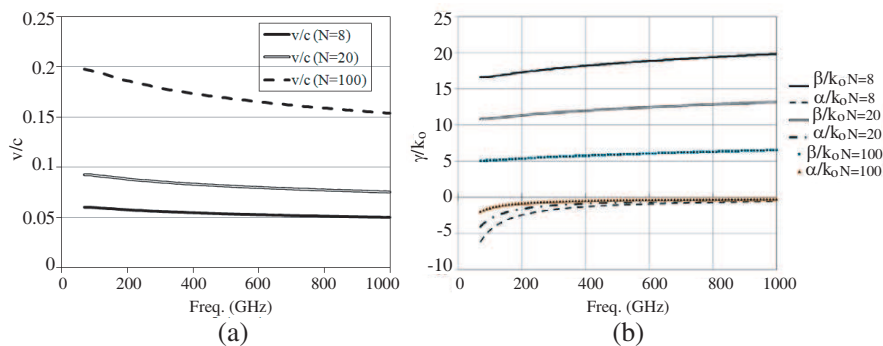


**Figure 6.** Surface wave propagation on CNT bundles of different values of  $N$ . The bundle is composed of armchair CNTs with lattice parameters  $m = n = 40$ . (a) Surface wave velocity compared with free space wave propagation. (b) Complex surface wave propagation constant compared with free space wave propagation constant.

space wave velocity and the complex propagation constant compared with the free space propagation constant on these CNT bundles. The surface wave velocity of an eight-carbon-nanotube bundle at 470 GHz is 0.056 which is the same reduction factor of the dipole length for  $N = 8$  in Fig. 2. Similarly, the same relations between reduction factors of the resonant dipole length for  $N = 20$  and  $N = 100$  shown in Fig. 2 and the corresponding surface wave velocity shown in Fig. 5(a) are obtained. These results show the quite relation between the resonant dipole length and the surface wave velocity on its arms. On the other hand, by studying the surface wave complex wave propagation constant, it can be noted that the attenuation coefficient increases by decreasing the operating frequency as shown in Fig. 6(b). The effect of this attenuation coefficient is negligible in the frequency range from 100 to 1000 GHz. Thus, the main behavior of the input impedance of the dipole antenna is nearly the same of traditional dipole antenna with taking into account scaling reduction factor due to the slow surface wave velocity. On the other hand, this attenuation coefficient has a moderate effect in the frequency band from 10 to 100 GHz. The resonance mechanism occurs when the incident wave at the feeding point adds constructively with the reflected wave from the dipole ends. However, in the band from 10 to 100 GHz, the wave propagating on the arms of the dipole is attenuated. Thus, the reflected wave does not add completely at the feeding point which means the inductive effect due to the delayed reflected signal does not compensate completely the capacitive effect of the dipole arms. This explains the capacitive behavior of CNT dipoles in Fig. 4. This behavior becomes clearer at lower frequency band from 1 GHz to 10 GHz where the attenuation coefficient is more increased. In this case, the wave propagating on the arms of the dipole is highly attenuated, such that the active part of the dipole is much smaller than the physical length of the dipole itself. Thus, the dipole would always be a short dipole in this case and it could not be resonant in any case. This result show that the advantage of size reduction combined with surface wave propagation can be used only in high frequency bands above 100 GHz.

#### 4. CONCLUSION

In this paper, the relation between the resonance mechanism of CNT bundle antenna and the surface wave propagation on this bundle structure is discussed. It is also shown that the complex surface wave propagation has a significant attenuation coefficient at lower frequency band. This attenuation coefficient introduces highly damping effect which reduces the active part of the dipole length. Thus, dipole would

be always below resonance in this case and its input impedance would be always capacitive. According to the results of complex surface wave propagation on CNT bundle it can be concluded that to obtain both resonance and size reduction, the lowest frequency that can be suitable for a CNT antenna is nearly 100 GHz. It is also shown that there is no relation between the resonant length and the approximate  $RLC$  representation of parallel wire CNT transmission line.

## REFERENCES

1. Iijima, S., "Helical microtabules of graphitic carbon," *Nature*, Vol. 354, 56–58, 1991.
2. Slepian, G. Y., S. A. Maksimenko, A. Lakhtakia, O. M. Yevtushenko, and A. V. Gusakov, "Electronic and electromagnetic properties of nanotubes," *Phys. Rev. B*, Vol. 57, 9485, 1998.
3. Slepian, G. Y., S. A. Maksimenko, A. Lakhtakia, O. M. Yevtushenko, and A. V. Gusakov, "Electrodynamics of carbon nanotubes: Dynamic conductivity, impedance boundary conditions, and surface wave propagation," *Phys. Rev. B*, Vol. 60, 17136–17149, 1999.
4. Miyamoto, Y., A. Rubio, S. G. Louie, and M. L. Cohen, "Self-inductance of chiral conducting nanotubes," *Phys. Rev. B*, Vol. 60, 13885, 1999.
5. Mikki, S. M. and A. A. Kishk, "A symmetry-based formalism for the electrodynamics of nanotubes," *Progress In Electromagnetics Research*, PIER 86, 111–134, 2008.
6. Hanson, G. W., "Fundamental transmitting properties of carbon nanotube antenna," *IEEE Trans. Antennas and Propagation*, Vol. 53, 3426–3435, 2005.
7. Burke, P. J., "Luttinger liquid theory as a model of Gigahertz electrical properties of carbon nanotubes," *IEEE Trans. Nanotechnology*, Vol. 1, 129–144, 2002.
8. Burke, P. J., "Corrections to Luttinger liquid theory as a model of Gigahertz electrical properties of carbon nanotubes," *IEEE Trans. Nanotechnology*, Vol. 3, 331, 2004.
9. Burke, P. J., "An RF circuit model for carbon nanotubes," *IEEE Trans. Nanotechnology*, Vol. 2, 55–58, 2003.
10. Burke, P. J., "Corrections to an RF circuit model for carbon nanotubes," *IEEE Trans. Nanotechnology*, Vol. 3, 331, 2004.
11. Chiariello, A. G., A. Maffucci, G. Miano, F. Villone, and W. Zamboni, "Metallic carbon nanotube interconnects, Part II: A

- transmission line model,” *IEEE Workshop on Signal Propagation on Interconnects*, 185–188, 2006.
12. Chiariello, A. G., A. Maffucci, G. Miano, F. Villone, and W. Zamboni, “Metallic carbon nanotube interconnects, Part I: A fluid model and a 3D integral formulation,” *IEEE Workshop on Signal Propagation on Interconnects*, 181–184, 2006.
  13. Maffucci, A. and G. Miano, “Electromagnetic and circuitual modeling of carbon nanotube interconnects,” *2nd Electronics System-integration Technology Conference*, 1051–1056, 2006.
  14. Miano, G., A. Maffucci, F. Villone, and W. Zamboni, “Frequency-domain modelling of nanoscale electromagnetic devices using a fluid model and an integral formulation,” *International Conference on Electromagnetics in Advanced Applications*, 233–236, 2007.
  15. Harrison, C. W., “Monopole with inductive loading,” *IEEE Trans. on Antennas and Propagation*, Vol. 11, 394–400, 1963.
  16. Hanson, G. W., “Current on an infinitely-long carbon nanotube antenna excited by a gap generator,” *IEEE Trans. Antennas and Propagation*, Vol. 54, 76–81, 2006.
  17. Hanson, G. W., “Radiation efficiency of nanoradius dipole antennas in the microwave and far-infrared regime,” *IEEE Antennas and Propagation Magazine*, Vol. 50, 66–77, 2008.
  18. Burke, P. J., S. Li, and Z. Yu, “Quantitative theory of nanowire and nanotube antenna performance,” *IEEE Trans. Nanotechnology*, Vol. 5, 314–334, 2006.
  19. Huang, Y., W.-Y. Yin, and Q. H. Liu, “Performance prediction of carbon nanotube bundle dipole antennas,” *IEEE Trans. Nanotechnology*, Vol. 7, 331–337, 2008.
  20. Slepian, G. Y., M. V. Shuba, A. M. Nemilentsau, and S. A. Maksimenko, “Electromagnetic theory of nanodimensional antennas for terahertz, infrared and optical regimes,” *12th International Conference on Mathematical Methods in Electromagnetic Theory*, 118–123, 2008.
  21. Fichtner, N., X. Zhou, and P. Russer, “Investigation of carbon nanotube antennas using thin wire integral equations,” *Adv. Radio Sci.*, Vol. 6, 209–211, 2008.
  22. Maffucci, A., G. Miano, G. Rubinacci, A. Tamburrino, and F. Villone, “Plasmonic, carbon nanotube and conventional nano-interconnects: A comparison of propagation properties,” *12th IEEE Workshop on Signal Propagation on Interconnects*, SPI 2008.

23. Shuba, M. V., S. A. Maksimenko, and A. Lakhtakia, "Electromagnetic wave propagation in an almost circular bundle of closely packed, metallic, carbon nanotubes," *Phys. Rev. B*, Vol. 76, No. 155407, 2007.
24. Hao, J. and G. W. Hanson, "Electromagnetic scattering from finite-length metallic carbon nanotubes in the lower IR bands," *Phys. Rev. B*, Vol. 74, No. 035119, 2006.
25. Elliot, R. S., *Antenna Theory and Design*, IEEE Press, 2003.
26. Li, W. and Y.-N. Wang, "Electromagnetic wave propagation in single-wall carbon nanotubes," *Physics Letters A*, Vol. 333, 303–309, 2004.
27. Pozar, D. M., *Microwave Engineering*, 3rd edition, Wiley, 2005.